


Invariance Property of the Fisher Information in Scattering Media

Michael Horodyski,¹ Dorian Bouchet,² Matthias Kühmayer,¹ and Stefan Rotter^{1,*}

¹*Institute for Theoretical Physics, Vienna University of Technology (TU Wien), 1040 Vienna, Austria*

²*Université Grenoble Alpes, CNRS, LIPhy, 38000 Grenoble, France*

 (Received 16 June 2021; accepted 27 October 2021; published 1 December 2021)

Determining the ultimate precision limit for measurements on a subwavelength particle with coherent laser light is a goal with applications in areas as diverse as biophysics and nanotechnology. Here, we demonstrate that surrounding such a particle with a complex scattering environment does, on average, not have any influence on the mean quantum Fisher information associated with measurements on the particle. As a remarkable consequence, the average precision that can be achieved when estimating the particle's properties is the same in the ballistic and in the diffusive scattering regime, independently of the particle's position within its nonabsorbing environment. This invariance law breaks down only in the regime of Anderson localization, due to increased C_0 -speckle correlations. Finally, we show how these results connect to the mean quantum Fisher information achievable with spatially optimized input fields.

DOI: 10.1103/PhysRevLett.127.233201

Precisely estimating the properties of subwavelength particles surrounded by scattering environments is a central aspect of many research areas, ranging from the measurement of the position and the mass of biological molecules [1,2] to the characterization of engineered nanostructures [3]. In these contexts, multiple scattering effects are usually seen as a major drawback, limiting the achievable precision in the estimation of observable parameters characterizing the particles. Nevertheless, it is also known that multiple scattering can sometimes be beneficial to optical imaging [4–7] as well as to single-particle localization and sensing [8–11], especially if prior knowledge on the scattering environment is available to the observer [12,13]. These insights naturally raise the question of how the presence of such a complex environment surrounding a subwavelength particle influences the information carried by the field scattered by the particle.

In recent years, the concept of Fisher information has enabled considerable progress in the precise characterization of subwavelength particles through optical measurements. Notably, this framework has been used to analytically derive fundamental limits on the achievable localization precision in the case of a fluorescent molecule located in free space [14–17] and for estimating the distance between two incoherent point sources [18–21]. In parallel, the influence of multiple scattering effects upon the Fisher information has been investigated based on numerical approaches for two spherical particles [22] as well as for larger ensembles of subwavelength particles [23]. These studies show that multiple scattering effects can either increase or decrease the achievable localization precision, depending on the microstructure of the scattering environment.

In this Letter, we uncover that the measurement precision achievable in scattering systems is actually subject to a counterintuitive invariance rule: the scattering environment surrounding a subwavelength particle does, on average, *not* influence *at all* the precision that can be achieved when estimating the properties of this particle (see Fig. 1). This result sheds new light on the possibility to use multiple-scattering effects for improving the measurement precision in complex systems. Moreover, the intimate connection between measurement and backaction [24] allows us to interpret this result also as an invariance rule for the average micromanipulation capabilities of waves in a scattering environment.

Specifically, we show that, in the canonical case of a flux-conserving system illuminated by a coherent field, the quantum Fisher information (QFI) as well as the associated quantum Cramér-Rao bound (QCRB)—averaged over

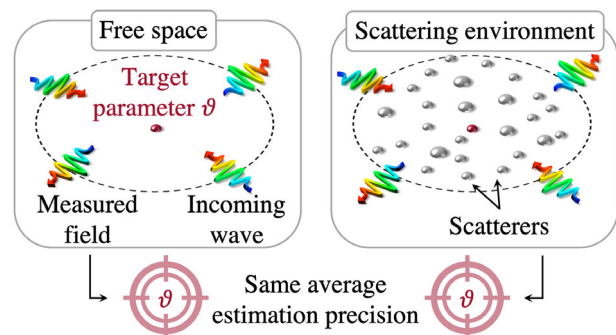


FIG. 1. Illustration of the concept. When illuminating a target (red) with coherent light (incoming arrows), the average precision that can be achieved, when estimating a property θ of the target, is the same whether the target is freely accessible (left) or embedded inside a nonabsorbing scattering environment (right).

configurations (or, equivalently, over frequencies) and over input angles—are both independent of the scattering strength of the environment surrounding the particle and of the particle’s position. This invariance law holds both in the ballistic and in the diffusive regime, whereas deviations are observed when Anderson localization sets in. Remarkably, in this case, both the average QFI and the average QCRB increase with the scattering strength of the medium as a result of C_0 -speckle correlations. In addition, we quantify the increase of the average QFI obtained when the incident field is spatially optimized using wavefront shaping techniques. Originating from a fundamental connection between the QFI [25], the local density of states (LDOS) [26] and the cross density of states (CDOS) [27], these results show that a simple fundamental law rules the ultimate precision limit achievable in estimating properties of a subwavelength particle using coherent light scattering.

The unavoidable presence of measurement noise imposes a lower limit on the precision that can be reached when using scattering measurements to estimate any given observable parameter θ , such as the position or the dielectric constant of a subwavelength particle. Here we consider the quantum fluctuations of the probe field as the relevant source of noise. The ultimate precision limit is then determined by the QFI defined as $\mathcal{I}_\theta = \text{Tr}(\hat{\rho}\hat{L}^2)$, where the density operator $\hat{\rho}$ describes the quantum state of the outgoing light and \hat{L} denotes the symmetric logarithmic derivative which is implicitly defined by $\hat{\rho}\hat{L} + \hat{L}\hat{\rho} = 2\partial_\theta\hat{\rho}$ [25,28]. The QCRB, which bounds the variance of unbiased estimators of θ , is simply expressed by $\Sigma_\theta = 1/\mathcal{I}_\theta$. This bound is reachable using an optimal detection scheme [28] together with an efficient estimator, which is easily found in the limit of small parameter variations [29]. The QFI thus provides us with a relevant metric to compare the estimation precision achievable with different probe fields and different scattering environments.

We consider that the measured field is in an N -mode coherent (Glauber) state $\hat{\rho} = |\{\alpha\}\rangle\langle\{\alpha\}|$, where $|\{\alpha\}\rangle = \prod_{k=1}^N |\alpha_k\rangle$ is given by the product of all the outgoing single-mode coherent states $|\alpha_k\rangle$. This state can also be described by a classical wave state $|v\rangle$ of modal coefficients $\{\alpha_1, \dots, \alpha_N\}$. When the classical scattering matrix S of the system is known, the QFI can be written in the following quadratic form [24]:

$$\mathcal{I}_\theta = 4\langle u|F_\theta|u\rangle, \quad (1)$$

where $F_\theta = \partial_\theta S^\dagger \partial_\theta S$ is the so-called Fisher information operator for the estimation of θ and $|u\rangle$ is the asymptotic wave state impinging on the system (such that $|v\rangle = S|u\rangle$). For any arbitrary incident wave state, Eq. (1) can thus be used to predict the QFI relative to the estimation of the parameter θ . The same expression can also be derived by calculating the classical Fisher information (CFI) [29]. Indeed, the CFI is equal to the QFI, provided that the

outgoing field is measured with an optimal detection scheme (such as a shot-noise-limited homodyne detector [24] in the context of coherent scattering measurements).

In the ideal case of a unitary S matrix, we can write $F_\theta = Q_\theta^2$, where $Q_\theta = -iS^{-1}\partial_\theta S$ denotes the generalized Wigner-Smith (GWS) operator [30,31]. Because of this connection, Eq. (1) can equivalently be used to quantify the perturbation applied to the parameter θ by the probe field. In the following, we will assume that the field is sufficiently weak, so that it does not significantly perturb the value of θ during the measurement process. This means that back-action noise, which can be significant in optomechanical systems [32,33], is neglected here.

The QFI averaged over all possible input fields is given by the following trace:

$$\mathcal{I}_\theta^{\text{avg}} = \frac{4}{N} \text{Tr}F_\theta = \frac{16}{N\Delta\theta^2} \text{Tr}[\text{Im}(G)\Delta H]^2, \quad (2)$$

where N is the total number of flux-carrying incoming channels, G is the Green’s function, $\Delta\theta$ is an infinitesimal variation of the parameter of interest, and ΔH is the corresponding change in the potential function $H(\mathbf{r}) \equiv k^2\epsilon(\mathbf{r})$. Here, k is the wave number and $\epsilon(\mathbf{r})$ describes the spatial distribution of the dielectric constant. We arrive at the second equality of Eq. (2) by using the expansion of the GWS operator $Q_\theta = 2V^\dagger G^\dagger \Delta H G V / \Delta\theta$, where V is the coupling matrix of the scattering system to the asymptotic channels [31]. Equation (2) expresses a system-specific connection between the externally accessible quantity $\mathcal{I}_\theta^{\text{avg}}$ and the local quantity $\text{Im}G$, which is proportional to the LDOS and CDOS at the target position. We will now show how this connection turns out to be extremely useful to demonstrate that the information is (on average) independent of system-specific parameters.

To this end, we now focus our attention on the estimation of a parameter θ characterizing a given subwavelength particle (the target), such as one of its coordinates (denoted by x_T) or its dielectric constant (denoted by ϵ_T). We also work under the assumption that the spatial distribution of the light field is statistically homogeneous and isotropic throughout the scattering medium (see [34], Sec. VI). This occurs when the scattering medium itself as well as the incoming light are statistically homogeneous and isotropic (i.e., for Lambertian illumination) [40,41]. We are then allowed to use the concept of the CDOS in order to quantify the effect of a small change in the position of the target on the QFI [27,42], resulting in a simple relation between $\mathcal{I}_\theta^{\text{avg}}$ and the LDOS $\rho(\mathbf{r}_T, k)$ at the location \mathbf{r}_T of the target (see [34], Sec. I). As a result, we find that the QFI averaged over all input channels (avg) and disorder configurations ($\langle\langle\cdots\rangle\rangle$) reads

$$\langle\mathcal{I}_\theta^{\text{avg}}\rangle = \frac{4B_\theta k^2 \pi^2}{N\epsilon_T^2} \langle\rho^2(\mathbf{r}_T, k)\rangle, \quad (3)$$

where the prefactor B_θ depends on the parameter of interest such that $B_x = k^2(\epsilon_T - 1)^2$ if $\theta = x_T$ and $B_\epsilon = 1$ if $\theta = \epsilon_T$.

Importantly, Eq. (3) links the average QFI directly to the square of the LDOS, thereby establishing that properties of particles that are placed at positions with an increased LDOS can be estimated more accurately. Our derivation also shows that a linear scaling of the LDOS with the QFI occurs in the case of considerably subunitary scattering matrices (see [34], Sec. II for a detailed derivation), as numerically observed in Ref. [23].

Under the isotropy assumption, we can use Weyl's law—which gives a simple expression for the average DOS in the asymptotic limit [43,44]—to estimate the average LDOS in 2D, $\langle \rho(\mathbf{r}_T, k) \rangle = Ak\epsilon_T/(2\pi)$, where A is the target's area. To use this approximation, however, we first have to relate $\langle \rho^2(\mathbf{r}_T, k) \rangle$ to $\langle \rho(\mathbf{r}_T, k) \rangle^2$. For this purpose, we use the connection between the variance of the LDOS and the C_0 -speckle correlations, $C_0 = \text{Var}[\rho(\mathbf{r}_T, k)]/\langle \rho(\mathbf{r}_T, k) \rangle^2$ [45,46], resulting in

$$\langle \mathcal{I}_\theta^{\text{avg}} \rangle = \frac{B_\theta k^4 A^2}{N} (1 + C_0). \quad (4)$$

The above equation establishes a counterintuitive invariance law: the average QFI is independent of the target's surrounding environment and of its position therein—provided that light scattering is in the ballistic or diffusive regime (for which $C_0 \simeq 0$, as numerically confirmed in [34], Sec. IV). Note that, while this invariance law is derived here for the two-dimensional scalar Helmholtz equation, the generality of the Fisher information operator and of the LDOS suggests that similar results could also be

derived with a three-dimensional, vectorial model. Indeed, the C_0 -speckle correlations show a similar behavior also in 3D, as we numerically demonstrate in [34], Sec. IV.

While we assumed that the probe field does not perturb the system, we can still calculate the average magnitude of this perturbation (e.g., a force) that we are neglecting. Indeed, for systems described by unitary scattering matrices, the GWS operator not only determines the QFI [24], but also quantifies the perturbation applied by the probe field upon the system parameter θ [31]. The average magnitude of the momentum transferred onto the particle as well as the average intensity focused onto it are thus also invariant quantities with respect to the scattering strength, in both the ballistic and diffusive regimes. Equation (3) also reveals an interesting conceptual connection to another known invariant quantity in wave scattering: the mean path length, which is related to the average density of states (DOS) in the whole scattering volume [40,47,48]. In a similar manner, we show here how the invariance of the mean path length in every subvolume [41] and an equivalent invariance of the LDOS emerge in the Fisher information.

To illustrate the implications of this invariance law, we choose the case of position estimations ($\theta = x_T$) for which we perform numerical simulations using a finite-element method (NGSolve) [49,50]. Our model system consists of a rectangular multimode waveguide of width W and length L , with hard walls at the top and bottom, and with openings to the left and right (see lower panels of Fig. 2). In this waveguide, we randomly place scatterers of different sizes

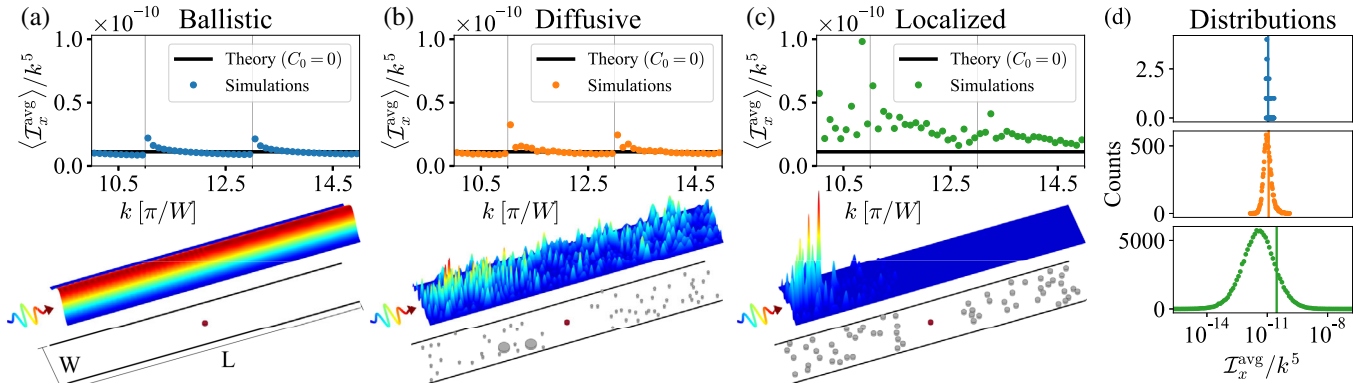


FIG. 2. Average QFI relative to the position x_T of a subwavelength particle in (a) the ballistic, (b) the diffusive, and (c) the localized regime. In the ballistic and diffusive regimes, numerical results are in excellent agreement with the theoretical predictions of Eq. (4), calculated for $C_0 = 0$ (black lines). In the localized regime, the C_0 -speckle correlations cannot be neglected, leading to an increase of the average QFI. In the diffusive and localized regimes, averages are calculated from 250 and 2500 different random configurations, respectively. Note that we approximated the number of transverse waveguide modes $N \simeq 2kW/\pi$ (grey vertical bars indicate odd mode openings). [(a)–(c), lower panels] The intensity distribution of the fundamental mode injected from the left lead is depicted (a) for an empty waveguide and for a given configuration of scatterers (grey cylinders) (b) with refractive index $n = 1.44$ or (c) with hard walls. The target (red cylinder) has refractive index $n = 1.44$ and is not shown to scale. As compared to the length L of the waveguide, the transport mean free path is $\ell_{tr} \approx 0.47L$ in the diffusive regime and the localization length is $\xi \approx 0.4L$ in the localized regime. (d) Distribution (on a logarithmic scale) of the average QFI $\mathcal{I}_\theta^{\text{avg}}$ for different disorder realizations, in the ballistic (blue), diffusive (orange) and localized (green) regimes, together with the value of $\langle \mathcal{I}_\theta^{\text{avg}} \rangle$ (vertical lines), which is averaged over disorder realizations.

and scattering cross sections in order to simulate disorder of adjustable scattering strength. We vary the wavelength between $\lambda = 2\pi/k \approx 0.2W$ and $\lambda \approx 0.13W$ such that between 10 and 14 transverse modes propagate inside the waveguide. The radius of the circular target is set to $R = W/200$, which is an order of magnitude smaller than the minimal wavelength considered here. For each configuration of the scatterers, after numerically calculating the scattering matrices associated with two close-by positions of the target, the derivative of scattering matrices with respect to the coordinate x_T is determined with a finite-difference scheme and the associated QFI is obtained using Eq. (1).

Using this numerical framework, we separately investigate the ballistic, diffusive, and localized regimes. For both ballistic and diffusive scattering [see Figs. 2(a) and 2(b)], our numerical results agree very well with the theoretical prediction of Eq. (4) when the C_0 -speckle correlation is neglected ($C_0 \simeq 0$). We note here that near-field interactions between scatterers can change the behavior of the C_0 -speckle correlations [51]—an effect we have explicitly excluded by not placing any scatterers within an exclusion square of sidelength W around the target (a discussion of numerical data without this exclusion region is provided in [34], Sec. IV). These results thus confirm that, even though the QFI strongly varies from configuration to configuration [see Fig. 2(d)], its average value stays remarkably insensitive to the scattering strength of the environment. Nevertheless, in the localized regime [Fig. 2(c)], C_0 cannot be neglected anymore and the average QFI increases. This trend can be explained by the estimate $C_0 \approx \pi/k\ell_{tr}$ [45], where ℓ_{tr} is the transport mean free path (see [34], Sec. IV for a numerical estimate of the C_0 correlation function). This increase of the average QFI in the localized regime can be understood from the fact that, while “typical” configurations are associated with a very low QFI, a few “resonant” configurations display an exceptionally large QFI [see Fig. 2(d)]—in analogy to the behavior of transport quantities [52]. Since these resonant scattering states exhibit very large dwell times, they are, however, also strongly affected by the absorption neglected here [53] (see [34], Sec. VII).

The average precision that can be achieved in an experiment is obtained by calculating $\langle \Sigma_\theta^{\text{avg}} \rangle$, which is the QCRB averaged over input fields and disorder configurations. This quantity is shown in Fig. 3 for the three scattering regimes previously studied (ballistic, diffusive, and localized). In the ballistic and diffusive regimes, that are easily accessible in optics, we observe that the average QCRB is constant regardless of the scattering strength of the environment, in the same way as the average QFI. Indeed, $\langle \Sigma_\theta^{\text{avg}} \rangle$ is here correctly estimated from linear propagation of error, i.e., $\langle \Sigma_\theta^{\text{avg}} \rangle \simeq 1/\langle \mathcal{I}_\theta^{\text{avg}} \rangle$. Since $C_0 \simeq 0$ in these regimes, we obtain

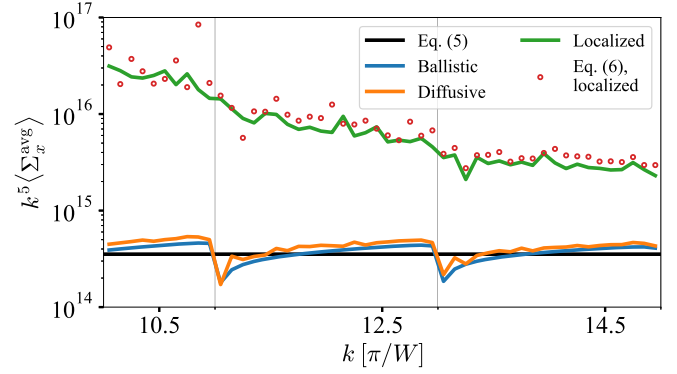


FIG. 3. Average QCRB $\langle \Sigma_\theta^{\text{avg}} \rangle$ relative to the position x_T for a subwavelength particle in the ballistic (blue), diffusive (orange), and localized (green) regime (grey vertical bars indicate odd mode openings in the waveguide). In the ballistic and diffusive regimes, that are most easily accessible in optics, numerical results (blue and orange lines) are in excellent agreement with the theoretical predictions of Eq. (5), demonstrating that the invariance law of the QFI leads to a similar invariance for the QCRB in these regimes. By contrast, in the localized regime, the average QCRB is drastically increased. In this regime, where linear propagation of error cannot be used, the average QCRB is correctly predicted using Eq. (6) (red dots).

$$\langle \Sigma_\theta^{\text{avg}} \rangle \simeq \frac{N}{B_\theta k^4 A^2}. \quad (5)$$

This expression shows that a simple invariance law also rules the average precision that can be achieved when estimating the properties of a subwavelength particle. This law yields the remarkable insight that the average precision achievable for a particle in free space neither increases nor decreases when this particle is placed in a complex, but nonabsorbing scattering environment.

Nevertheless, this invariance law does not apply to the localized regime, in which the average QCRB drastically increases with the scattering strength of the environment (see Fig. 3). In this regime, linear propagation of error cannot be used, and $\langle \Sigma_\theta^{\text{avg}} \rangle \neq 1/\langle \mathcal{I}_\theta^{\text{avg}} \rangle$. A connection can, however, still be made using the observation that both quantities follow a log-normal distribution [23] (see [34], Sec. V for a detailed derivation), resulting in

$$\langle \Sigma_\theta^{\text{avg}} \rangle = \frac{\langle \text{Tr}^2 F_\theta \rangle}{4N \langle \text{Tr} F_\theta \rangle^3}. \quad (6)$$

This expression not only involves the variance of the LDOS but also higher moments of the LDOS and the CDOS, which can be numerically estimated with a maximum likelihood method. The theoretical prediction obtained using this procedure is in excellent agreement with numerical observations, as shown in Fig. 3.

Lastly, we also investigate the maximal QFI $\mathcal{I}_\theta^{\text{max}}$ as achievable by wavefront shaping techniques [24,54,55].

We find that also this quantity follows, on average, a simple relationship, $\langle T_\theta^{\max} \rangle = p_\theta N \langle T_\theta^{\text{avg}} \rangle$. Here p_θ is a constant that depends on the parameter of interest with $p_\varepsilon = 1$ and $p_x \in [0.5, 1]$ (see [34], Sec. III for a more detailed discussion).

To summarize, we derive a universal invariance property for the average QFI and for the average QCRB applicable to both the ballistic and diffusive regimes. This result implies that coherent light fields can be used to measure the position or the dielectric constant of a subwavelength particle with an average precision that is the same, regardless of the scattering strength of the surrounding environment. In the regime of Anderson localization, however, the increased scattering strength simultaneously enhances the average QFI and the average QCRB. Although these results are derived here for a two-dimensional model system in the present work, extensions to all physical scenarios featuring a linear wave equation should be possible (including 3D vector waves). Moreover, by averaging not over disorder but over a sufficiently broad frequency range, our results should be extendable to targets in nonuniform engineered media and correlated disorders, such as photonic crystals [56], Lévy glasses [57], hyperuniform media [58], and inhomogeneously disordered materials [59] for which correlations in the disorder lead to a modified value of C_0 [45].

Support by the Austrian Science Fund (FWF) under Project No. P32300 (WAVELAND) is gratefully acknowledged. The computational results were achieved using the Vienna Scientific Cluster (VSC).

* stefan.rotter@tuwien.ac.at

- [1] R. W. Taylor and V. Sandoghdar, *Nano Lett.* **19**, 4827 (2019).
- [2] G. Young and P. Kukura, *Annu. Rev. Phys. Chem.* **70**, 301 (2019).
- [3] N. G. Orji, M. Badaroglu, B. M. Barnes, C. Beitia, B. D. Bunday, U. Celano, R. J. Kline, M. Neisser, Y. Obeng, and A. E. Vladar, *National electronics review* **1**, 532 (2018).
- [4] F. Simonetti, *Phys. Rev. E* **73**, 036619 (2006).
- [5] J. Girard, G. Maire, H. Giovannini, A. Talneau, K. Belkebir, P. C. Chaumet, and A. Sentenac, *Phys. Rev. A* **82**, 061801 (R) (2010).
- [6] J. A. Newman, Q. Luo, and K. J. Webb, *Phys. Rev. Lett.* **116**, 073902 (2016).
- [7] Q. Luo and K. J. Webb, *Phys. Rev. Research* **2**, 033148 (2020).
- [8] R. Berkovits and S. Feng, *Phys. Rev. Lett.* **65**, 3120 (1990).
- [9] R. Berkovits, *Phys. Rev. B* **43**, 8638 (1991).
- [10] P. N. den Outer, T. M. Nieuwenhuizen, and A. Lagendijk, *J. Opt. Soc. Am. A* **10**, 1209 (1993).
- [11] J. Berk and M. R. Foreman, *ACS Photonics* **8**, 2227 (2021).
- [12] A. Szameit, Y. Shechtman, E. Osherovich, E. Bullkich, P. Sidorenko, H. Dana, S. Steiner, E. B. Kley, S. Gazit, T. Cohen-Hyams, S. Shoham, M. Zibulevsky, I. Yavneh, Y. C. Eldar, O. Cohen, and M. Segev, *Nat. Mater.* **11**, 455 (2012).
- [13] T. Zhang, C. Godavarthi, P. C. Chaumet, G. Maire, H. Giovannini, A. Talneau, M. Allain, K. Belkebir, and A. Sentenac, *Optica* **3**, 609 (2016).
- [14] R. J. Ober, S. Ram, and E. S. Ward, *Biophys. J.* **86**, 1185 (2004).
- [15] K. I. Mortensen, L. S. Churchman, J. A. Spudich, and H. Flyvbjerg, *Nat. Methods* **7**, 377 (2010).
- [16] H. Deschout, F. C. Zanacchi, M. Młodzianoski, A. Diaspro, J. Bewersdorf, S. T. Hess, and K. Braeckmans, *Nat. Methods* **11**, 253 (2014).
- [17] M. P. Backlund, Y. Shechtman, and R. L. Walsworth, *Phys. Rev. Lett.* **121**, 023904 (2018).
- [18] S. Ram, E. S. Ward, and R. J. Ober, *Proc. Natl. Acad. Sci. U.S.A.* **103**, 4457 (2006).
- [19] M. Tsang, R. Nair, and X.-M. Lu, *Phys. Rev. X* **6**, 031033 (2016).
- [20] M. Pařr, B. Stoklasa, Z. Hradil, L. L. Sánchez-Soto, and J. Rehacek, *Optica* **3**, 1144 (2016).
- [21] Y. Zhou, J. Yang, J. D. Hassett, S. M. H. Rafsanjani, M. Mirhosseini, A. N. Vamivakas, A. N. Jordan, Z. Shi, and R. W. Boyd, *Optica* **6**, 534 (2019).
- [22] A. Sentenac, C.-A. Guérin, P. C. Chaumet, F. Drsek, H. Giovannini, N. Bertaux, and M. Holschneider, *Opt. Express* **15**, 1340 (2007).
- [23] D. Bouchet, R. Carminati, and A. P. Mosk, *Phys. Rev. Lett.* **124**, 133903 (2020).
- [24] D. Bouchet, S. Rotter, and A. P. Mosk, *Nat. Phys.* **17**, 564 (2021).
- [25] C. W. Helstrom, *J. Stat. Phys.* **1**, 231 (1969).
- [26] W. L. Barnes, *J. Mod. Opt.* **45**, 661 (1998).
- [27] A. Cazé, R. Pierrat, and R. Carminati, *Phys. Rev. Lett.* **110**, 063903 (2013).
- [28] S. L. Braunstein, C. M. Caves, and G. J. Milburn, *Ann. Phys. (N.Y.)* **247**, 135 (1996).
- [29] H. L. V. Trees, K. L. Bell, and Z. Tian, *Detection Estimation and Modulation Theory, Part I* (Wiley, New York, 2013).
- [30] P. Ambichl, A. Brandstötter, J. Böhm, M. Kühmayer, U. Kuhl, and S. Rotter, *Phys. Rev. Lett.* **119**, 033903 (2017).
- [31] M. Horodyski, M. Kühmayer, A. Brandstötter, K. Pichler, Y. V. Fyodorov, U. Kuhl, and S. Rotter, *Nat. Photonics* **14**, 149 (2020).
- [32] A. A. Clerk, M. H. Devoret, S. M. Girvin, F. Marquardt, and R. J. Schoelkopf, *Rev. Mod. Phys.* **82**, 1155 (2010).
- [33] D. Mason, J. Chen, M. Rossi, Y. Tsaturyan, and A. Schliesser, *Nat. Phys.* **15**, 745 (2019).
- [34] See Supplemental Material at <http://link.aps.org/supplemental/10.1103/PhysRevLett.127.233201> for detailed derivations and additional numerical results, which includes Refs. [35–39].
- [35] P. de Vries, D. V. van Coevorden, and A. Lagendijk, *Rev. Mod. Phys.* **70**, 447 (1998).
- [36] P. del Hougne, K. B. Yeo, P. Besnier, and M. Davy, *Phys. Rev. Lett.* **126**, 193903 (2021).
- [37] V. V. Marinyuk, *Phys. Rev. A* **104**, 023517 (2021).
- [38] S. Blanco and R. Fournier, *Europhys. Lett.* **61**, 168 (2003).
- [39] C. Beenakker and P. Brouwer, *Physica (Amsterdam)* **9E**, 463 (2001).

- [40] R. Savo, R. Pierrat, U. Najar, R. Carminati, S. Rotter, and S. Gigan, *Science* **358**, 765 (2017).
- [41] O. Bénichou, M. Coppey, M. Moreau, P.H. Suet, and R. Voituriez, *Europhys. Lett.* **70**, 42 (2005).
- [42] A. Canaguier-Durand, R. Pierrat, and R. Carminati, *Phys. Rev. A* **99**, 013835 (2019).
- [43] H. Weyl, *Nachr. Ges. Wiss. Göttingen, Math.-Phys. Kl.* **1911**, 110 (1911), <http://eudml.org/doc/58792>.
- [44] *Mathematical Analysis of Evolution, Information, and Complexity*, 1st ed., edited by W. Arendt and W. P. Schleich (Wiley, New York, 2009).
- [45] B. A. van Tiggelen and S. E. Skipetrov, *Phys. Rev. E* **73**, 045601(R) (2006).
- [46] A. Cazé, R. Pierrat, and R. Carminati, *Phys. Rev. A* **82**, 043823 (2010).
- [47] R. Pierrat, P. Ambichl, S. Gigan, A. Haber, R. Carminati, and S. Rotter, *Proc. Natl. Acad. Sci. U.S.A.* **111**, 17765 (2014).
- [48] M. Davy, M. Kühmayer, S. Gigan, and S. Rotter, *Commun. Phys.* **4**, 85 (2021).
- [49] J. Schöberl, *Comput. Visualization Sci.* **1**, 41 (1997).
- [50] J. Schöberl, C++11 implementation of finite elements in NGSolve, ASC Report, Institute for Analysis and Scientific Computing, Vienna University of Technology, 2014.
- [51] R. Sapienza, P. Bondareff, R. Pierrat, B. Habert, R. Carminati, and N.F. van Hulst, *Phys. Rev. Lett.* **106**, 163902 (2011).
- [52] K. Y. Bliokh, Y. P. Bliokh, and V. D. Freilikher, *J. Opt. Soc. Am. B* **21**, 113 (2004).
- [53] K. Y. Bliokh, Y. P. Bliokh, V. Freilikher, A. Z. Genack, B. Hu, and P. Sebbah, *Phys. Rev. Lett.* **97**, 243904 (2006).
- [54] A. P. Mosk, A. Lagendijk, G. Lerosey, and M. Fink, *Nat. Photonics* **6**, 283 (2012).
- [55] S. Rotter and S. Gigan, *Rev. Mod. Phys.* **89**, 015005 (2017).
- [56] A. F. Koenderink, A. Lagendijk, and W. L. Vos, *Phys. Rev. B* **72**, 153102 (2005).
- [57] P. Barthelemy, J. Bertolotti, and D. S. Wiersma, *Nature (London)* **453**, 495 (2008).
- [58] S. Torquato and F. H. Stillinger, *Phys. Rev. E* **68**, 041113 (2003).
- [59] Y. Huang, C. Tian, V. A. Gopar, P. Fang, and A. Z. Genack, *Phys. Rev. Lett.* **124**, 057401 (2020).